Electrical transport properties of $La_{1-x}Sr_xCoO_3$ thin films

Bin Liu,[1] Yiqian Wang,[1,a)] Guiju Liu,[1] Honglei Feng,[1] Huaiwen Yang,[2] and Jirong Sun[2]
[1]*College of Physics and The Cultivation Base for State Key Laboratory, Qingdao University, No. 308, Ningxia Road, Qingdao 266071, People's Republic of China*
[2]*Beijing National Laboratory for Condensed Matter Physics, Institute of Physics, Chinese Academy of Sciences, Beijing 100080, People's Republic of China*

(Received 22 July 2016; accepted 4 October 2016; published online 18 October 2016)

The electrical transport properties of $La_{1-x}Sr_xCoO_3$ (LSCO) thin films were investigated in this paper. As x increased up to 0.3, the electrical transport mechanism transferred from variable range hopping to double-exchange and the film simultaneously turned from an insulator into a conductor. Different from the bulk materials, the maximum conductivity of the film appeared at $x = 0.3$. A novel electrical transport model was proposed to explain this unconventional phenomenon. Besides, the effects of doped Sr and oxygen vacancies on the electrical transport properties were clarified by investigated the transport behaviors of the $LaCoO_3$, $La_{0.7}S_{0.3}CoO_3$, and $La_{0.7}S_{0.3}CoO_{3-\delta}$ films. We found that, when Sr was doped into the $LaCoO_3$ film, the insulating film turns into a conductor; when oxygen atoms were removed from the $La_{0.7}S_{0.3}CoO_3$ film, the conducting film goes back to an insulator. Our work could shed light on the electrical transport mechanism of the LSCO films. *Published by AIP Publishing.*
[http://dx.doi.org/10.1063/1.4964946]

I. INTRODUCTION

The perovskite oxides have attracted considerable interest since Jonker[1] and Van Santen[2] discovered the strong correlation between ferromagnetism and metallic conductivity in the doped manganites in 1950. Later, Zener[3] proposed a mechanism of double-exchange (DE) interaction, in which two degenerated configurations Mn^{3+}-$O^{2-}$$Mn^{4+}$ and Mn^{4+}-$O^{2-}$$Mn^{3+}$ in doped manganites are connected by a so-called DE matrix element. Because of strong Hund's coupling, the transfer matrix element has a finite value only when the core spins of Mn ions are aligned ferromagnetically, leading to a ferromagnetic conducting ground state.

In the past decades, extensive studies about bulk samples $La_{1-x}Sr_xCoO_3$ (LSCO) were performed due to their fascinating electrical transport properties.[4–7] In 1996, Mineshige *et al.*[8,9] studied the relationship between the electrical transport properties and the content of Sr for bulk LSCO. They found that, at $x \sim 0.25$, the Co-O distance and Co-O-Co angle of this system showed an abrupt decrease and increase with increasing x, respectively, inducing an insulator to a metal transition. Then, Kozuka *et al.*[10] observed that, in the bulk LSCO, the metal-insulator transition (MIT) appears at $x \sim 0.2$ and the maximum conductivity is obtained at $x = 0.5$. We noted that most previous reports just focused on bulk LSCO and ascribed the MIT to the variation of the Co-O-Co bond distance and angle.

For the LSCO films, some excellent work about the electrical transport mechanism, particularly on the effects of substrate[11–13] and film thickness,[14] has been carried out. However, up to now, no work on the relation between Sr content, MIT and maximal conductivity has been reported for the LSCO films. In this work, we investigated the conductivity of the LSCO films with $0 \le x \le 0.5$. Different from bulk samples, the MIT occurs at $x = 0.3$ and the best conductivity no longer appears at half doping. To understand the origin of the MIT and the maximal conductivity, an electrical transport model for the LSCO film is proposed. Moreover, the effects of oxygen vacancies and doped Sr on conductivity are synchronously studied and an insulator-metal-insulator (I-M-I) transition is observed in the $LaCoO_3$-based thin films.

II. EXPERIMENTAL SECTION

The LSCO films with $0 \le x \le 0.5$ were epitaxially grown on the (001) $SrTiO_3$ (STO) and (001) $LaAlO_3$ (LAO) substrates using the pulsed laser deposition (PLD) technique. The target was prepared by the solid state reaction from the ceramic powders of La_2O_3, $SrCO_3$, and Co_2O_3. The wavelength of the excimer laser was 248 nm, the laser energy density was 1.5 J/cm^2, and the repetition rate was 1 Hz. During the deposition process, the substrate was maintained at 800 °C and the oxygen pressure was kept at 50 Pa. The film thickness was ~50 nm, determined by deposition time. After the deposition, the films were naturally cooled down to room temperature at 50 Pa. To investigate the effect of oxygen vacancies on transport properties, the as-prepared $La_{0.7}Sr_{0.3}CoO_3$ films were further annealed in an oxygen atmosphere of 10^{-4} Pa at 300 °C for 1 min and then naturally cooled to room temperature at 10^{-4} Pa.

Specimens for transmission electron microscopy (TEM) examinations were prepared in cross-sectional orientations ([010] zone axis for STO substrates) using the conventional techniques of mechanical polishing and ion thinning. The

a)Author to whom correspondence should be addressed. Electronic mail: yqwang@qdu.edu.cn

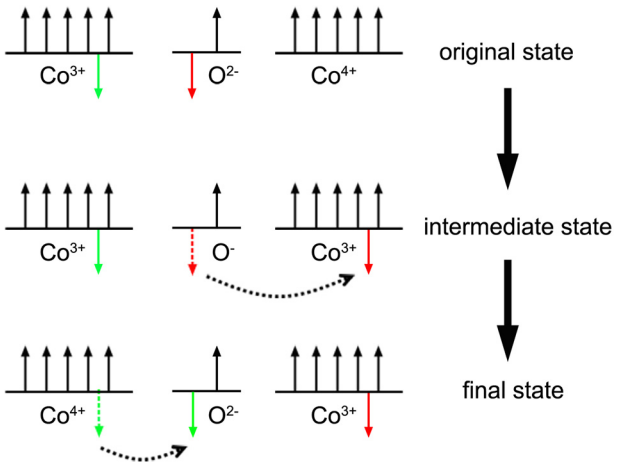

FIG. 1. DE process in Sr-doped $LaCoO_3$ film.

ion milling was performed using a Gatan Model 691 precision ion polishing system (PIPS). The bright-field (BF) imaging, selected-area electron diffraction (SAED), and high-resolution TEM (HRTEM) examinations were carried out on a JEOL JEM 2100 F electron microscope operated at 200 kV. The film structure was analyzed by X-ray diffraction (Bruker X-ray diffractometer, $\lambda = 1.5406$ Å). The film morphology was examined by the atomic force microscopy (Seiko SPI 3800 N) at the ambient conditions. The chemical compositions of LSCO films prepared at different oxygen pressures were determined using energy dispersive X-ray spectroscopy (EDS) in the JEOL JEM2100F TEM and X-ray photoelectron spectroscopy (XPS) on the Thermo Scientific ESCALAB 250Xi. The transport properties were characterized by a physical property measurement system (PPMS) with a temperature down to 2 K and a magnetic field up to 13 T. The applied magnetic field was parallel to the sample surface as well as the current direction.

III. RESULTS AND DISCUSSION

In this work, all the LSCO films with $0 \le x \le 0.5$ were prepared by the PLD technique. From the X-ray diffraction and atomic force microscopy results (in supplementary material), we confirm that all the deposited films are well crystallized and have a smooth surface. The temperature-dependent resistivity (R vs T) of the LSCO/STO ($0 \le x \le 0.5$) thin films is shown in Fig. 2(a). At $x = 0$, the film is insulating, which is consistent with the previous reports.[15–17] The ln$R$ vs $T^{-1/4}$ curve in Fig. 2(b) fits well to the equation of $\rho(T) = \rho_0 \exp(T_0/T)^{1/4}$,[18] which means that the electrical transport mechanism of the LCO film is a three-dimensional variable range hopping (VRH). With increasing x, the resistivity of the film rapidly decreases and eventually the metallic R vs T curves appear for the films with the Sr content of $0.3 \le x \le 0.5$. It is known that the DE interaction is responsible for the ferromagnetic ordering and metallic conduction in manganites.[3] As shown in Fig. 1, the DE theory is applicable to LSCO. Similar to the manganites, in the final state, the LSCO is ferromagnetic and conducting. From the fitting curves of ln$R$ vs $T^{-1/4}$ shown in Figs. 2(b) and 2(c), we draw a conclusion that, as x increases up to 0.3, the electrical transport mechanism transfers from VRH to DE and the insulating films turn into metallic. For comparison purposes, the R vs T curves of the LSCO/LAO films are also investigated and the results are shown in Fig. 3. It is clear that, in low-doping levels ($0 \le x < 0.3$), the films are insulating and the dominant transport mechanism is VRH, while, in high-doping levels ($0.3 \le x \le 0.5$), the dominant transport mechanism is DE and the films turn into metallic.

According to Zener, the materials (both bulk and film samples) possess the best electrical conductivity only when the DE between the Co^{3+} and Co^{4+} cations is maximized. That is why the maximum conductivity is observed at $x = 0.5$ for the bulk materials.[10] However, from the R vs T curves (shown in Figs. 2(a) and 3(a)), the conductivity of $La_{0.7}Sr_{0.3}CoO_3$ films are better than $La_{0.5}Sr_{0.5}CoO_3$ films. To explain this unconventional phenomenon, HRTEM examinations of the LSCO ($x = 0.3$) films were performed and the results are shown in Fig. 4(a). A typical modulated structure with a periodicity twice the original lattice parameter is observed in A sites (A-O plane of ABO_3). In the SAED pattern of the film (inserted in Fig. 4(a)), all the superlattice diffraction spots labelled with white arrows only appear at 1/2 positions between the (001) fundamental reflections, which means that all the stripes are parallel to the film surface. It has been proved that the chemical arrangement in the film can be tuned by the epitaxial strain imposed by the substrate, changes in oxygen content and cation mobility, and the oxygen-vacancy ordering.[20] Unavoidably, the oxygen vacancies were introduced into the film when deposited onto the substrate and the nominal valence of the Co ions depends not

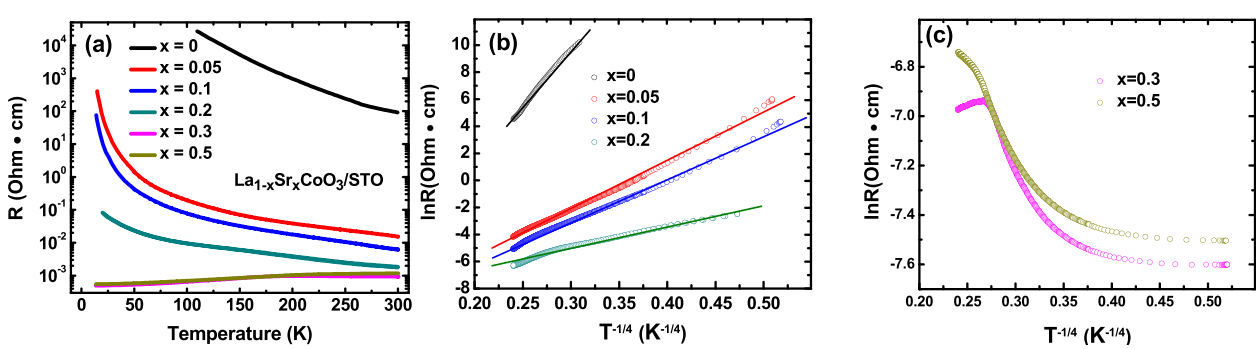

FIG. 2. (a) Temperature dependence of resistivity of LCO and different LSCO films grown on STO;[19] (b) and (c) plot of lnR against $T^{-1/4}$ of the resistivity data from (a).

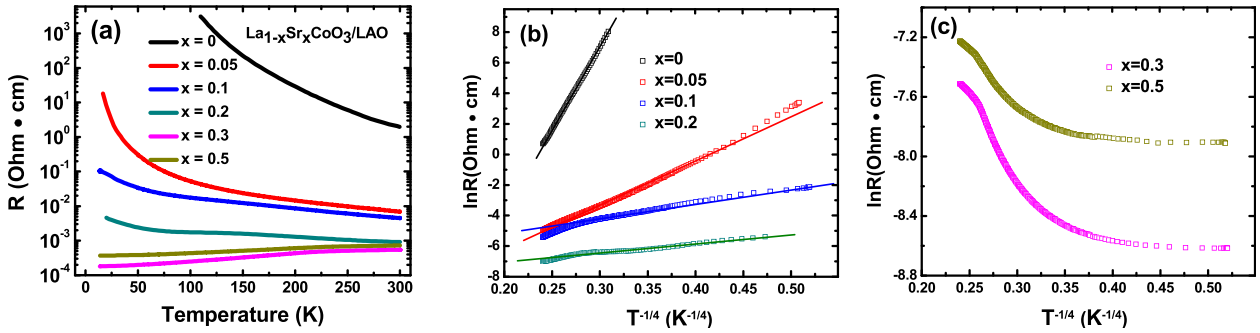

FIG. 3. (a) Temperature dependence of resistivity of LCO and different LSCO films grown on LAO;[19] (b) and (c) plot of lnR against $T^{-1/4}$ of the resistivity data from (a).

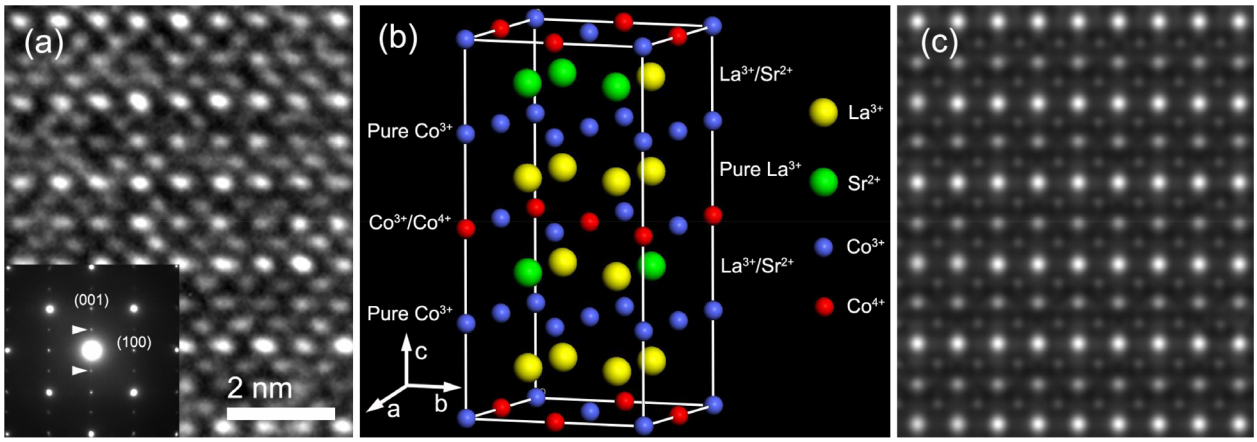

FIG. 4. (a) Typical HRTEM image of $La_{0.7}Sr_{0.3}CoO_{2.975}$ film grown on STO, and the inset shows the SAED pattern of the film (two arrows denote the superlattice reflections); (b) atomic model of the $La_{0.7}Sr_{0.3}CoO_{2.975}$ film with oxygen atoms omitted; and (c) simulated HRTEM image with $\Delta f = -113.0$ nm and $t = 15.3$ nm.

only on the Sr content but also on the oxygen concentration. The oxygen contents of the LSCO films with different doping contents of Sr were measured by EDS and XPS (in supplementary material), and the results are summarized in Table I. Consistent with the previous report of Iwasaki *et al.*,[21] the oxygen vacancies content (δ) of the $La_{0.7}Sr_{0.3}CoO_3$ film is ~0.025. Its ionic states can be determined to be $La^{3+}_{0.7}Sr^{2+}_{0.3}Co^{3+}_{0.75}Co^{4+}_{0.25}O^{2-}_{2.975}$ and its crystal structure is shown in Fig. 4(b). In this model, the Co-O planes are divided into pure Co^{3+} planes and Co^{3+}/Co^{4+} mixed planes. In the pure Co^{3+} planes, all the Co are trivalent and in the Co^{3+}/Co^{4+} mixed planes all the cations are arranged at random. To keep the charge balance, of course, the cations in La^{3+}/Sr^{2+} mixed planes are randomly arranged. To distinguish these configurations, both pure and mixed atomic planes are illustrated in Fig. 4(b). Systematic HRTEM simulations of this model were performed, and one simulated image with $\Delta f = -113.0$ nm (defocus value) and $t = 15.3$ nm (thickness) shown in Fig. 4(c) agrees well with the experimental results. In this image, the modulated structure with a periodicity of two-fold the original unit lattice distance is located at A sites, which is derived from the pure La^{3+} planes and the mixed La^{3+}/Sr^{2+} planes. However, in B sites, no modulated stripe is observed. We deduce that the mixed arranged Co^{3+}/Co^{4+} cations and small amount of oxygen vacancies (0.833%) cannot be reflected in the HRTEM image. Based on this result and the DE theory, a novel electrical transport model is proposed. In our experiment, we measured the resistivity along the film surface, i.e., along the mixed Co^{3+}/Co^{4+} planes. In those planes, the ratio of Co^{3+}/Co^{4+} is ~1 and the DE between Co^{3+} and Co^{4+} cations is maximized, which induces the best electrical conductivity. However, for the Sr

TABLE I. Oxygen vacancies content and ionic structure of the LSCO films with $0 \le x \le 0.5$.

Sr Content	Oxygen-vacancy content	Oxygen-vacancy percentage (%)	Ionic structure for LSCO films
0	0.002	0.067	$La^{3+}_{1.00}Co^{3+}_{2.996}Co^{2+}_{0.004}O^{2-}_{2.998}$
0.05	0.005	0.167	$La^{3+}_{0.95}Sr^{2+}_{0.05}Co^{3+}_{0.96}Co^{4+}_{0.04}O^{2-}_{2.995}$
0.1	0.010	0.333	$La^{3+}_{0.90}Sr^{2+}_{0.10}Co^{3+}_{0.92}Co^{4+}_{0.08}O^{2-}_{2.990}$
0.2	0.015	0.500	$La^{3+}_{0.80}Sr^{2+}_{0.20}Co^{3+}_{0.83}Co^{4+}_{0.17}O^{2-}_{2.985}$
0.3	0.025	0.833	$La^{3+}_{0.70}Sr^{2+}_{0.30}Co^{3+}_{0.75}Co^{4+}_{0.25}O^{2-}_{2.975}$
0.5	0.040	1.333	$La^{3+}_{0.50}Sr^{2+}_{0.50}Co^{3+}_{0.58}Co^{4+}_{0.42}O^{2-}_{2.960}$

doping levels lower or higher than 0.3, the Co^{3+} and Co^{4+} cations are not equal in the mixed planes and the DE is no longer maximized. That is why the maximum conductivity appears at $x = 0.3$ in the LSCO films. The low temperature resistivity of conducting LSCO films is shown in the supplementary material. The residual resistivity is lower than that of thin films ($1 \times 10^{-3}\,\Omega\,cm$) and even closed to that of bulk samples ($3 \times 10^{-4}\,\Omega\,cm$) in the previous report.[14]

The HRTEM examinations of the LSCO ($x = 0.1$ and 0.5) films grown on STO were also performed, and the results were shown in Fig. 5. A modulated structure with a periodicity of three-fold, the original unit lattice distance was observed in the HRTEM image of the $La_{0.9}Sr_{0.1}CoO_{2.990}$ film (shown in Fig. 5(a)). Its SAED pattern also supported this result as two additional dots appeared at 1/3 positions between the (001) reflections. Its periodicity is quite different to the $La_{0.7}Sr_{0.3}CoO_{2.975}$ film. In other words, except the substrate, oxygen content and cation mobility, the chemical arrangement in the film can also be tuned by the doping content. We have proved that the pure La^{3+} planes are brighter than the mixed La^{3+}/Sr^{2+} planes in the HRTEM image.[22,23] Thus, this modulated structure is derived from one pure La^{3+} planes and two mixed La^{3+}/Sr^{2+} planes. To keep the original ratio ($x = 0.1$), in the mixed La^{3+}/Sr^{2+} planes, La^{3+}:Sr^{2+} is 20:3. Considering the oxygen vacancy, Co^{3+}:Co^{4+} should be larger than 20:3 in the mixed Co^{3+}/Co^{4+} planes. The DE between Co^{3+} and Co^{4+} cations is not enough to make the films ($x \leq 0.1$) conducting. Fig. 5(b) shows the HRTEM image of the $La_{0.5}Sr_{0.5}CoO_{2.960}$ film. A modulated structure of two-fold the original unit lattice is observed. Considering its original ratio, the ordered structure has a layered arrangement of La-Co-Sr-Co, which is consistent with the previous literature.[24] As La^{3+} and Sr^{2+} cations are arranged in order, the Co^{3+} and Co^{4+} cations are also in order. However, highly ordered arrangement of Co^{3+} and Co^{4+} cations is not good for the electronic transport. Thus, the best conductivity no longer appears at $x = 0.5$ in the LSCO films.

From the above, we know that the insulating LCO film turned into conducting after Sr-doping and the $La_{0.7}Sr_{0.3}CoO_3$ film has the best conductivity. Irrespective of the oxygen vacancies, the maximum conductivity should appear at $x = 0.25$ in the ideal LSCO films, which is consistent with the results of Mineshige *et al.*[8,9] To investigate the effect of doped Sr and oxygen vacancy on the electrical transport properties of LSCO film, the stoichiometric LCO and $La_{0.7}Sr_{0.3}CoO_3$ films were epitaxially deposited on STO and LAO and the $La_{0.7}Sr_{0.3}CoO_{3-\delta}$ film was prepared by annealing the resultant $La_{0.7}Sr_{0.3}CoO_3$ film in vacuum. Fig. 6 shows the typical BF TEM images of these films grown on STO. The thickness of all the films is ~50 nm. The LCO and $La_{0.7}Sr_{0.3}CoO_3$ films are homogeneous, and their surfaces are smooth. However, for the $La_{0.7}Sr_{0.3}CoO_{3-\delta}$ film, its surface is no longer flat. The LCO film is insulating (shown in Fig. 7(a)), which is an indication that the film is nearly stoichiometric without substantial deviation from stoichiometry.[25] As considerable Sr ($x = 0.3$) is doped into LCO, the film becomes conducting. We fitted the curves of $\ln R$ vs $T^{-1/4}$ for the LCO films before and after doping, and the results are shown in Figs. 7(b) and 7(c). It is consistent with our previous conclusion that the electrical transport mechanism of the film transfers from VRH to DE after the Sr-doping. However, after annealing the $La_{0.7}Sr_{0.3}CoO_3$ film in the vacuum, oxygen atoms are removed from it and the conducting film becomes insulating. We have mentioned that the most basic requirement of DE interaction is the matrix element that arises via the transfer of an electron from Co^{3+} to the central O^{2-} with the simultaneous transfer from O^{2-} to Co^{4+}. As oxygen vacancies are introduced into the film, the Co^{4+} cations are reduced into Co^{3+} and the transition bridge (O^{2-}) is destroyed. The conducting film turns into an insulator. Interestingly, in the process of doping Sr into LCO film and removing oxygen from $La_{0.7}Sr_{0.3}CoO_3$ film, an insulator-metal-insulator (I-M-I) transition occurs. As the I-M-I transition is also observed in the films grown on LAO

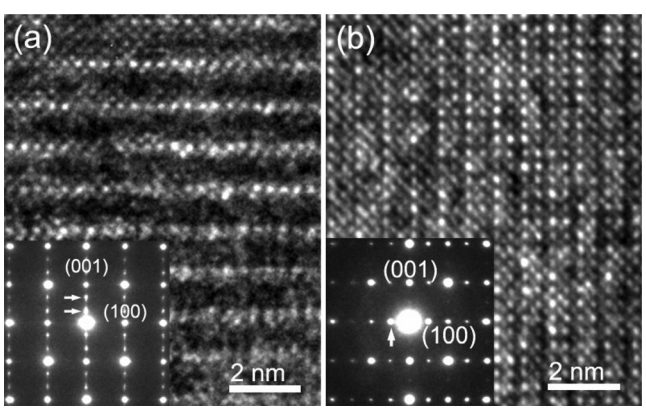

FIG. 5. Typical HRTEM images of $La_{0.9}Sr_{0.1}CoO_{2.990}$ (a) and $La_{0.5}Sr_{0.5}CoO_{2.960}$ (b) films grown on STO. Insets show the corresponding SAED patterns (the arrows denote the superlattice reflections).

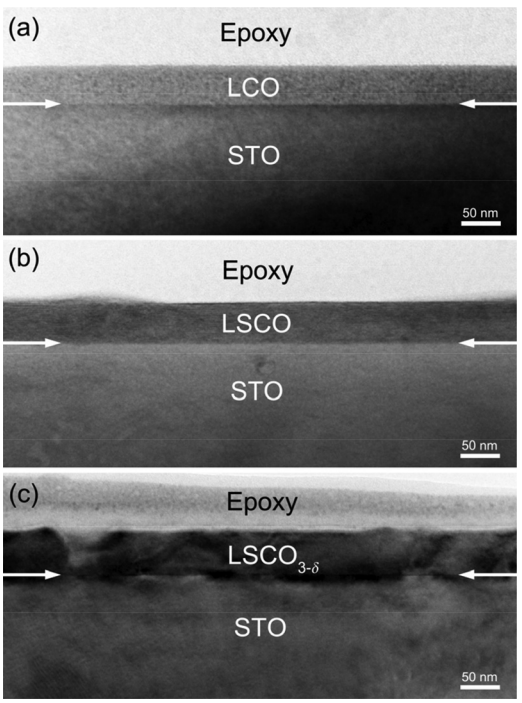

FIG. 6. Typical BF TEM images of (a) $LaCoO_3$, (b) $La_{0.7}Sr_{0.3}CoO_3$, and (c) $La_{0.7}Sr_{0.3}CoO_{3-\delta}$ films grown on STO.

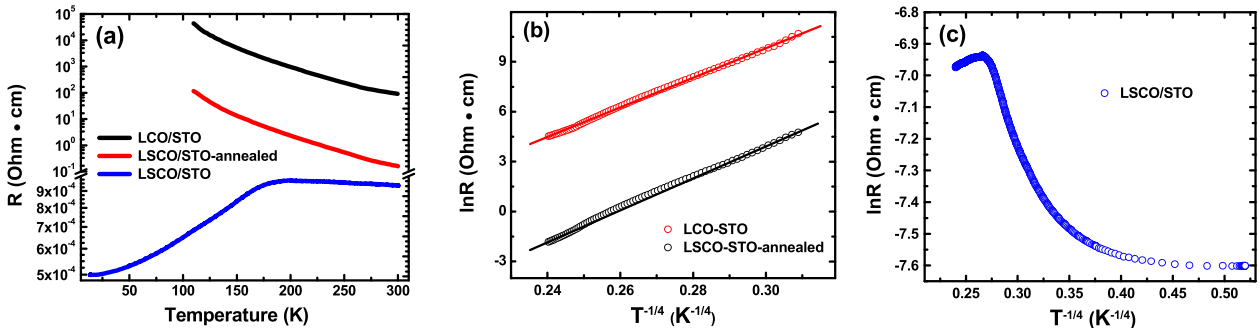

FIG. 7. (a) Temperature dependence of resistivity for $LaCoO_3$, $La_{0.7}Sr_{0.3}CoO$, and $La_{0.7}Sr_{0.3}CoO_{3-\delta}$ films grown on STO; (b) and (c) plot of lnR against $T^{-1/4}$ of the resistivity data from (a).

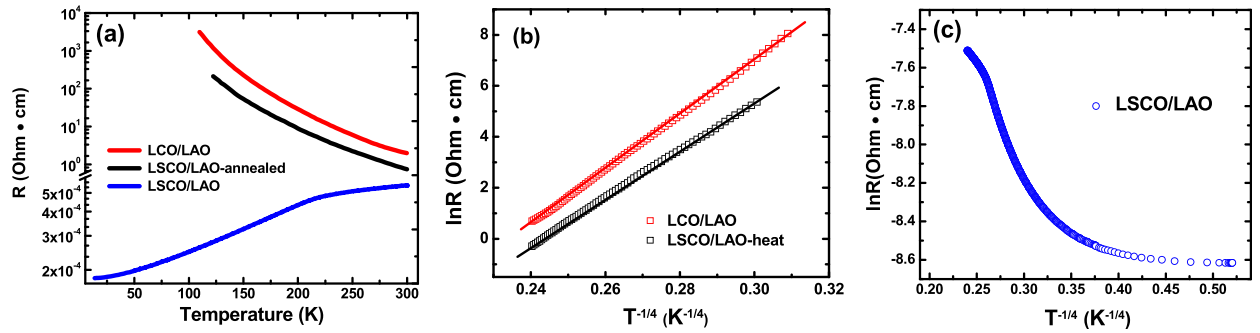

FIG. 8. (a) Temperature dependence of resistivity for $LaCoO_3$, $La_{0.7}Sr_{0.3}CoO$, and $La_{0.7}Sr_{0.3}CoO_{3-\delta}$ films grown on LAO; (b) and (c) plot of lnR against $T^{-1/4}$ of the resistivity data from (a).

substrate (shown in Fig. 8), we can confirm that interfacial strain between the film and the substrate does not play a significant role in the transition.

IV. CONCLUSIONS

In this work, we presented a systematic study to decipher the roles of doped Sr and oxygen vacancies in the electrical transport mechanism of $La_{1-x}Sr_xCoO_3$ films. As doped Sr increased from 0 to ~0.3, the electrical transport mechanism of the films transferred from VRH to DE simultaneously with a transformation of insulating into metallic. A novel electrical transport model was proposed to explain why the best conductivity appeared at $x = 0.3$ for the $La_{1-x}Sr_xCoO_3$ films. From the R vs T curves and fitted lnR against $T^{-1/4}$ curves of LCO, $La_{0.7}Sr_{0.3}CoO_3$ and $La_{0.7}Sr_{0.3}CoO_{3-\delta}$ films, we found that the DE interaction is interrupted as the introduced oxygen vacancies reduce the Co^{4+} into Co^{3+} and destroy the exchange bridge, and the film goes back to an insulator.

SUPPLEMENTARY MATERIAL

See supplementary material for the XRD, AFM, EDS, and XPS results and the low-temperature residual resistivity.

ACKNOWLEDGMENTS

The authors would like to thank the financial support from the National Key Basic Research Development Program of China (Grant No. 2012CB722705), the National Natural Science Foundation of China (Grant No. 10974105), and the Program for Foreign Cultural and Educational Experts (Grant Nos. GDW20143500163 and GDW20133400112). Y. Q. Wang would also like to thank the financial support from the Top-notch Innovative Talent Program of Qingdao City (Grant No. 13-CX-8) and the Taishan Scholar Program of Shandong Province, China.

[1]G. H. Jonker and J. H. Van Santen, Physica (Amsterdam) **16**, 337 (1950).
[2]J. H. Van Santen and G. H. Jonker, Physica (Amsterdam) **16**, 599 (1950).
[3]C. Zener, Phys. Rev. **82**, 403 (1951).
[4]A. N. Petrov, O. F. Kononchuk, A. V. Andreev, V. A. Cherepanov, and P. Kofstad, Solid State Ionics **80**, 189 (1995).
[5]C. X. Li, M. Gao, C. J. Li, W. Zhou, G. J. Yang, and Y. Y. Wang, Mater. Trans. **47**, 1654 (2006).
[6]Q. Y. Xie, Z. P. Wu, X. S. Wu, and W. S. Tan, J. Alloys Compd. **474**, 81 (2009).
[7]R. X. Smith, M. J. R. Hoch, W. G. Moulton, P. L. Kuhns, A. P. Reyes, and G. S. Boebinger, Phys. Rev. B **86**, 054428 (2012).
[8]A. Mineshige, M. Inaba, T. Yao, Z. Ogumi, K. Kikuchi, and M. Kawase, J. Solid State Chem. **121**, 423 (1996).
[9]A. Mineshige, M. Kobune, S. Fujii, Z. Ogumi, M. Inaba, T. Yao, and K. Kikuchi, J. Solid State Chem. **142**, 374 (1999).
[10]H. Kozuka, H. Yamada, T. Hishida, K. Yamagiwa, K. Ohbayashia, and K. Koumoto, J. Mater. Chem. **22**, 20217 (2012).
[11]A. D. Rata, A. Herklotz, K. Nenkov, L. Schultz, and K. Dorr, Phys. Rev. Lett. **100**, 076401 (2008).
[12]Q. X. Zhu, W. Wang, X. Q. Zhao, X. M. Li, Y. Wang, H. S. Luo, H. L. W. Chan, and R. K. Zheng, J. Appl. Phys. **111**, 103702 (2012).
[13]F. Wu, X. M. Li, W. D. Yu, X. D. Gao, and X. Cao, Solid State Commun. **145**, 178 (2008).
[14]Z. Othmen, A. Schulman, K. Daoudi, M. Boudard, C. Acha, H. Roussel, M. Oueslatia, and T. Tsuchiya, Appl. Surf. Sci. **306**, 60 (2014).
[15]I. Lucas, J. M. Vila-Fungueirino, P. Jimenez-Cavero, B. Rivas-Murias, C. Magen, L. Morellon, and F. Rivadulla, ACS Appl. Mater. Interfaces **6**, 21279 (2014).

[16]T. Shang, Q. F. Zhan, H. L. Yang, Z. H. Zuo, Y. L. Xie, Y. Zhang, L. P. Liu, B. M. Wang, Y. H. Wu, S. Zhang, and R. W. Li, Phys. Rev. B **92**, 165114 (2015).
[17]H. Takahashi, F. Munakata, and M. Yamanaka, Phys. Rev. B **53**, 3731 (1996).
[18]G. J. Snyder, R. Hiskes, S. DiCarolis, M. R. Beasley, and T. H. Geballe, Phys. Rev. B **53**, 14434 (1996).
[19]H. W. Yang, Ph.D. thesis, Institute of Physics, Chinese Academy of Sciences, Beijing, 2015.
[20]W. Donner, C. L. Chen, M. Liu, A. J. Jacobson, Y. L. Lee, M. Gadre, and D. Morgan, Chem. Mater. **23**, 984 (2011).
[21]K. Iwasaki, T. Ito, T. Nagasaki, Y. Arita, M. Yoshino, and T. Matsui, J. Solid State Chem. **181**, 3145 (2008).
[22]B. Liu, G. J. Liu, H. L. Feng, C. Wang, H. W. Yang, and Y. Q. Wang, Mater. Des. **89**, 715 (2016).
[23]B. Liu, Y. Q. Wang, G. J. Liu, H. L. Feng, H. W. Yang, X. Y. Xue, and J. R. Sun, Phys. Rev. B **93**, 094421 (2016).
[24]Z. L. Wang and J. M. Zhang, Phys. Rev. B **54**, 1153 (1996).
[25]N. Biškup, J. Salafranca, V. Mehta, M. P. Oxley, Y. Suzuki, S. J. Pennycook, S. T. Pantelides, and M. Varela, Phys. Rev. Lett. **112**, 087202 (2014).